

Extended Boost Quasi-Z-Source Inverters: Possibilities and Challenges

D. Vinnikov, I. Roasto, T. Jalakas, S. Ott

Department of Electrical Drives and Power Electronics, Tallinn University of Technology,
Ehitajate tee 5, 19086 Tallinn, Estonia, phone: +372 6203705, e-mail: dmitri.vinnikov@ieee.org

crossref <http://dx.doi.org/10.5755/j01.eee.112.6.444>

Introduction

Quasi-Z-source inverter (qZSI) is a new promising power conversion technology perfectly suitable for interfacing of renewable (i.e., photovoltaic, wind turbines) and alternative (i.e., fuel cells) energy sources [1-3]. The qZSI has the following advantages:

- Boost-buck function by the one-stage conversion;
- Continuous input current (input current never drops to zero, thus featuring the reduced stress of the input voltage source, which is especially topical in such demanding applications as power conditioners for fuel cells and solar panels);
- Excellent reliability due to the shoot-through withstanding capability;
- Low or no in-rush current during start up;
- Low common-mode noise.

However, the efficiency and voltage gain of the qZSI are limited and comparable with the conventional system of a voltage source inverter with the auxiliary step-up DC/DC converter in the input stage [4]. The concept of extending the qZSI gain without increasing the number of active switches was recently proposed by several authors [5-8]. These new converter topologies are commonly referred to as the *extended boost qZSI* or *cascaded qZSI* and could be generally classified as capacitor assisted and diode assisted topologies [5]. In this paper different extended boost qZSIs with continuous input current will be presented, analyzed and compared. Moreover, some problematic issues of these converters will be pointed out and discussed.

Extended Boost qZSI – Basic Topologies

It should be noted here that this paper provides a general coverage of the extended boost voltage-fed qZSIs with continuous input current. All the topologies to be discussed and analyzed have a common property - the input inductor L_1 that buffers the source current. It means that during the continuous conduction mode (CCM) the input current of the converter never drops to zero, thus featuring the reduced stress of the input voltage source.

Capacitor Assisted Extended Boost qZSI. The investigated topologies are presented in Fig. 1. The basic topology of a capacitor assisted extended boost qZSI (CAEB qZSI, Fig. 1a) could be derived by the adding of one diode (D_2), one inductor (L_3) and two capacitors (C_3 and C_4) to the traditional qZSI with continuous input current [6-8]. The modified topology of a capacitor assisted extended boost qZSI (MCAEB qZSI) could be derived from the CAEB qZSI simply by the changing of the connection points of capacitors C_2 and C_3 , as shown in Fig. 1b.

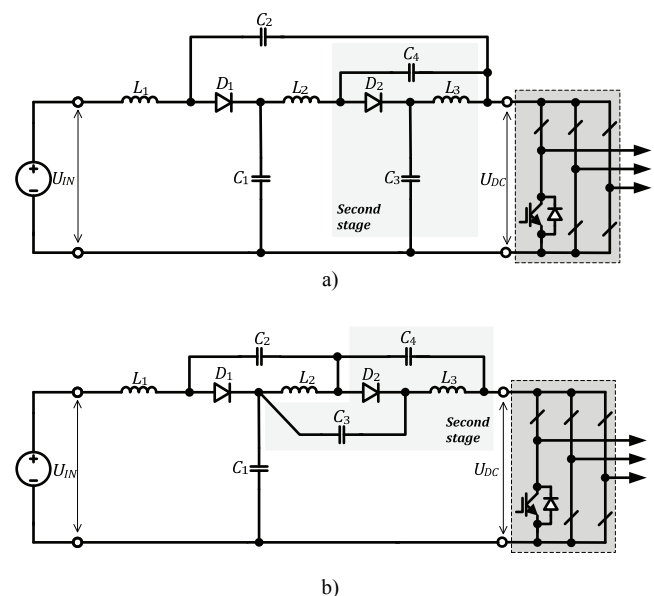


Fig. 1. Capacitor assisted extended boost qZSI topologies: basic CAEB qZSI (a) and MCAEB qZSI (b)

Diode Assisted Extended Boost qZSI. The investigated topologies are presented in Fig. 2. The basic topology of a diode assisted extended boost qZSI (DAEB qZSI, Fig. 2a) could be derived by the adding of one capacitor (C_3), one inductor (L_3) and two diodes (D_2 and D_3) to the traditional qZSI with continuous input current. The modified topology of a diode assisted extended boost qZSI (MDAEB qZSI) could be derived from the DAEB qZSI simply by the

changing of the connection points of the capacitor C_3 , as shown in Fig. 1b.

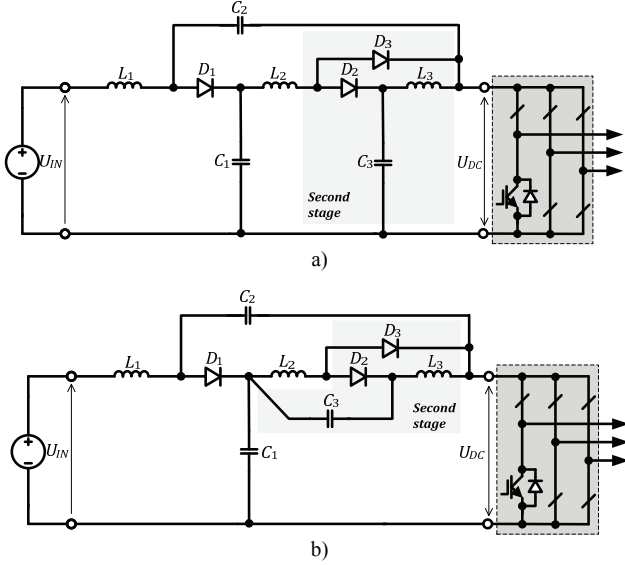


Fig. 2. Diode assisted extended boost qZSI topologies: basic DAEB qZSI (a) and MDAEB qZSI (b)

Steady state analysis of extended boost qZSI topologies

Generally, the topologies shown in Figs. 1 and 2 could be represented by the PWM inverter coupled with the cascaded qZS-network. In the same manner as the traditional qZSI, the extended boost qZSI has two types of operational states at the dc side: the non-shoot-through states (i.e., the six active states and two conventional zero states of the traditional three-phase voltage source inverter (VSI)) and the shoot-through state (i.e., both switches in at least one phase conduct simultaneously) [7–9]. To simplify our analysis the inverter bridge was replaced by a switch S (Fig. 3). When the switch S is closed, the shoot-through state occurs and the converter performs the voltage boost action. When the switch S is open, the active (non-shoot-through) state emerges and previously stored magnetic energy in turn provides the boost of voltage seen on the load terminals.

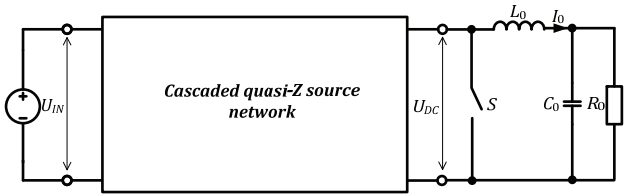


Fig. 3. Simplified power circuit of the extended boost qZSI used in the analysis

The operating period of the qZS-converter in the CCM basically consists of a shoot-through state t_s and an active state t_A

$$T = t_A + t_s. \quad (1)$$

(1) could also be represented as

$$\frac{t_A}{T} + \frac{t_s}{T} = D_A + D_S = 1, \quad (2)$$

where D_A and D_S are the duty cycles of an active and shoot-through states, correspondingly.

Capacitor Assisted Extended Boost qZSI. Fig. 4 shows the equivalent circuits of the CAEB qZSI operating in the CCM for the shoot-through (a) and active (b) states.

From the equivalent circuit of the CAEB qZSI during the shoot-through state (Fig. 4a), the voltage of the inductors can be represented as:

$$u_{L1} = U_{IN} + U_{C2}; \quad (3)$$

$$u_{L2} = U_{C4} + U_{C1}; \quad (4)$$

$$u_{L3} = U_{C3}. \quad (5)$$

During the active (non-shoot-through) state (Fig. 3b), the voltage of the inductors can be represented as

$$u_{L1} = U_{IN} - U_{C1}; \quad (6)$$

$$u_{L2} = U_{C4} - U_{C2} = U_{C1} - U_{C3}; \quad (7)$$

$$u_{L3} = -U_{C4}. \quad (8)$$

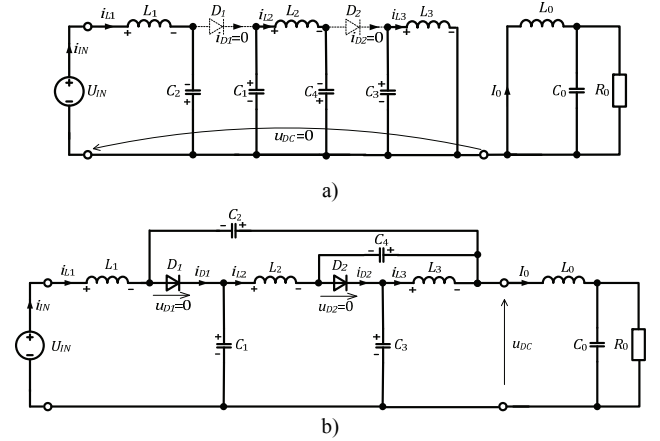


Fig. 4. Equivalent circuits of the CAEB qZSI: during the shoot-through state (a) and during the active (non-shoot-through) state (b)

At the steady state the average voltage of the inductors over one operating period is zero. Considering that fact and defining the shoot-through duty cycle as D_S and the non-shoot-through duty cycle as $(1-D_S)$, the voltages of capacitors $C_1 \dots C_4$ can be found

$$U_{C1} = U_{IN} \frac{1-2D_S}{1-3D_S}; \quad U_{C2} = U_{IN} \frac{2D_S}{1-3D_S}; \quad U_{C3} = U_{IN} \frac{1-D_S}{1-3D_S};$$

$$U_{C4} = U_{IN} \frac{D_S}{1-3D_S}.$$

The peak DC-link voltage is

$$\hat{u}_{DC} = U_{C1} + U_{C2} = U_{C3} + U_{C4} = U_{IN} \frac{1}{1-3D_S}. \quad (9)$$

The boost ratio of the input voltage is

$$B = \frac{\hat{u}_{DC}}{U_{IN}} = \frac{1}{1-3D_S}. \quad (10)$$

Fig. 5 shows the equivalent circuits of the modified

CAEB qZSI operating in the CCM for the shoot-through (a) and active (b) states.

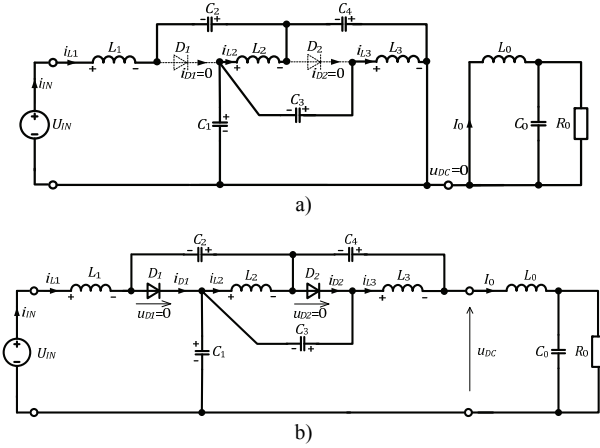


Fig. 5. Equivalent circuits of the MCAEB qZSI: during the shoot-through state (a) and during the active (non-shoot-through) state (b)

From the equivalent circuit of the MCAEB qZSI during the shoot-through state (Fig. 5a), the voltage of the inductors can be represented as:

$$u_{L1} = U_{IN} + U_{C2} + U_{C4}; \quad (11)$$

$$u_{L2} = U_{C1} + U_{C4}; \quad (12)$$

$$u_{L3} = U_{C1} + U_{C3}. \quad (13)$$

During the active (non-shoot-through) state (Fig. 5b) the voltage of the inductors can be represented as:

$$u_{L1} = U_{IN} - U_{C1}; \quad (14)$$

$$u_{L2} = -U_{C3} = -U_{C2}; \quad (15)$$

$$u_{L3} = -U_{C4}. \quad (16)$$

The voltages of capacitors \$C_1...C_4\$:

$$U_{C1} = \frac{1-2D_S}{1-3D_S} \cdot U_{IN}, \quad U_{C2} = U_{C3} = U_{C4} = \frac{D_S}{1-3D_S} \cdot U_{IN}.$$

The peak DC-link voltage across the switch \$S\$ is

$$\hat{u}_{DC} = U_{C1} + U_{C2} + U_{C4} = U_{IN} \frac{1}{1-3D_S}. \quad (17)$$

The boost ratio of the input voltage of the MCAEB topology is the same as of CAEB qZSI (10).

Diode Assisted Extended Boost qZSI. Fig. 6 shows the equivalent circuits of the DAEB qZSI operating in the CCM for the shoot-through (a) and active (b) states.

From the equivalent circuit of the DAEB qZSI during the shoot-through state (Fig. 6a), the voltage of the inductors can be represented as:

$$u_{L1} = U_{IN} + U_{C2}; \quad (18)$$

$$u_{L2} = U_{C1}; \quad (19)$$

$$u_{L3} = U_{C3}. \quad (20)$$

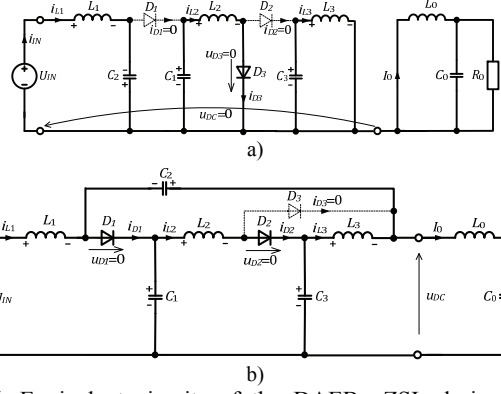


Fig. 6. Equivalent circuits of the DAEB qZSI: during shoot-through state (a) and during the active (non-shoot-through) state (b)

During the active (non-shoot-through) state (Fig. 6b), the voltage of the inductors can be represented as:

$$u_{L1} = U_{IN} - U_{C1}; \quad (21)$$

$$u_{L2} = -U_{C3}; \quad (22)$$

$$u_{L3} = U_{C3} - U_{C2}. \quad (23)$$

The voltages of capacitors \$C_1...C_3\$

$$U_{C1} = U_{IN} \frac{D_S^2 - 2D_S + 1}{D_S^2 - 3D_S + 1}, \quad U_{C2} = U_{IN} \frac{2D_S - D_S^2}{D_S^2 - 3D_S + 1},$$

$$U_{C3} = U_{IN} \frac{1 - D_S}{D_S^2 - 3D_S + 1}.$$

The peak DC-link voltage is

$$\hat{u}_{DC} = U_{C1} + U_{C2} = U_{IN} \frac{1}{D_S^2 - 3D_S + 1}. \quad (24)$$

The boost ratio of the input voltage is

$$B = \frac{\hat{u}_{DC}}{U_{IN}} = \frac{1}{D_S^2 - 3D_S + 1}. \quad (25)$$

Fig. 7 shows the equivalent circuits of the MDAEB qZSI operating in the CCM for the shoot-through (a) and active (b) states. From the equivalent circuit of the modified MDAEB qZSI during the shoot-through state (Fig. 7a), the voltage of the inductors could be represented as:

$$u_{L1} = U_{IN} + U_{C2}; \quad (26)$$

$$u_{L2} = U_{C1}; \quad (27)$$

$$u_{L3} = U_{C3} + U_{C1}. \quad (28)$$

During the active (non-shoot-through) state (Fig. 7b), the voltage of the inductors could be represented as:

$$u_{L1} = U_{IN} - U_{C1}; \quad (29)$$

$$u_{L2} = -U_{C3}; \quad (30)$$

$$u_{L3} = U_{C3} - U_{C2}. \quad (31)$$

The voltages of capacitors $C_1 \dots C_3$ are

$$U_{C1} = U_{IN} \frac{D_S^2 - 2D_S + 1}{D_S^2 - 3D_S + 1}; \quad U_{C2} = U_{IN} \frac{2D_S - D_S^2}{D_S^2 - 3D_S + 1};$$

$$U_{C3} = U_{IN} \frac{D_S - D_S^2}{D_S^2 - 3D_S + 1}.$$

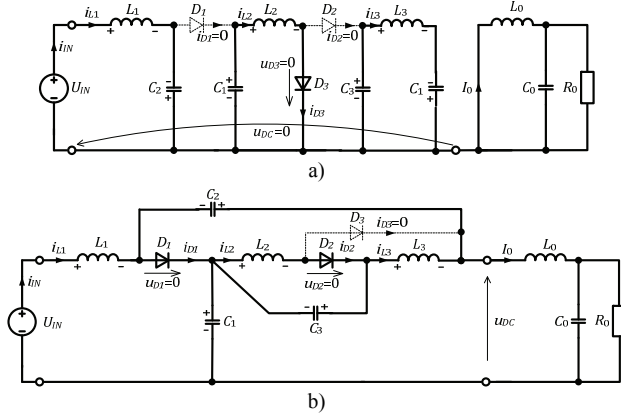


Fig. 7. Equivalent circuits of the MDAEB qZSI: during the shoot-through state (a) and during the active (non-shoot-through) state (b)

The peak DC-link voltage is

$$\hat{u}_{DC} = U_{C1} + U_{C2} = U_{IN} \frac{1}{D_S^2 - 3D_S + 1}. \quad (32)$$

The boost ratio of the input voltage of the MDAEB topology is the same as of DAEB qZSI (25).

Comparison of operating properties of different extended boost qZSI topologies

In order to verify theoretical assumptions a number of simulations were performed by the help of PSIM simulation software. The proposed extended boost qZSI topologies were evaluated with the switching frequency $f=30$ kHz and shoot-through duty cycle $D_S=0.167$. The input voltage was set at 30 V and the load resistor selected was 5 Ω . To simplify the analysis losses in the components were neglected. Capacitors and inductors selected for the qZS-networks have the following parameters: $L_1 \dots L_3 = 65$ μ H; $C_1 \dots C_4 = 180$ μ F.

Capacitor Assisted Extended Boost qZSI. Fig. 8 shows the general operating waveforms of the CAEB and MCAEB qZSI topologies. As expected, both converters operate normally, producing twofold boost of the input voltage ($U_{IN}=30$ V, $U_{DC}=60$ V, Fig. 8a and Fig. 8b). Moreover, the topologies ensure the continuous input current (Fig. 8a) in the CCM.

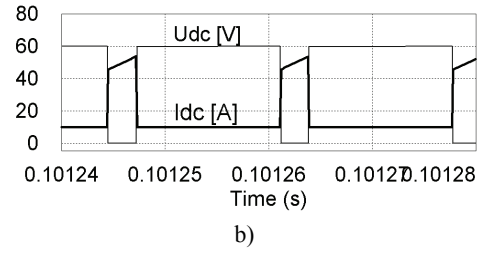
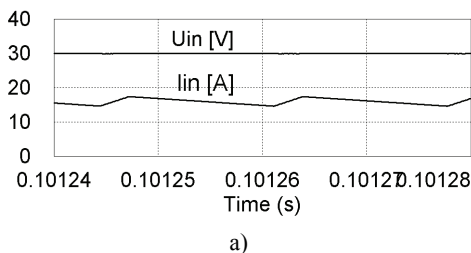


Fig. 8. Simulated waveforms of the CAEB and MCAEB qZSI topologies: input voltage and current (a) and DC-link voltage and current (b)

The average values of capacitor voltages of the CAEB and MCAEB qZSI topologies obtained during the simulations are compared in Table 1. It shows that by changing the interconnection points of capacitors C_2 and C_3 , as in Fig. 1b, the operating voltages of the capacitor C_3 were reduced by five times. Moreover, the voltages of capacitors $C_2 \dots C_4$ are equalized now.

Table 1. Comparison of operating voltages of capacitors in CAEB and MCAEB qZSI topologies

Capacitors	Operating voltages	
	CAEB qZSI	MCAEB qZSI
C_1	39.9 V	40.4 V
C_2	19.8 V	9.8 V
C_3	49.6 V	9.8 V
C_4	10.1 V	10.3 V

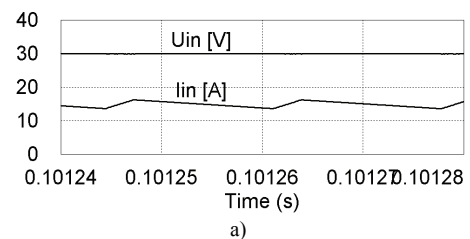
Diode Assisted Extended Boost qZSI. Fig. 9 shows the general operating waveforms of the DAEB and MDAEB qZSI topologies. Both converters operate normally, producing the demanded boost of the input voltage ($U_{IN}=30$ V; $U_{DC}=57$ V, Figs. 9a and 9b). As expected, both topologies ensure the continuous input current (Fig. 9a) in the CCM.

The average values of capacitor voltages of the DAEB and MDAEB qZSI topologies obtained during the simulations are compared in Table 2. It shows that by changing the interconnection points of the capacitor C_3 (Fig. 2b), its operating voltage could be decreased by more than six times.

Table 2. Comparison of operating voltages of capacitors in DAEB and MDAEB qZSI topologies

Capacitors	Operating voltages	
	DAEB qZSI	MDAEB qZSI
C_1	39.5 V	39.5 V
C_2	17.2 V	17.4 V
C_3	47.4 V	7.7 V

In Fig. 10 the operating waveforms of the diode D_3 (see Fig. 2 for the details) are presented. It is shown that for the discussed application the low-voltage low-power fast recovery or the Schottky diode could be used.



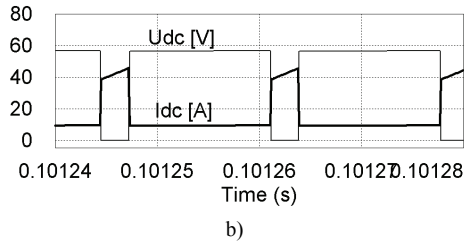


Fig. 9. Simulated waveforms of the DAEB and MDAEB qZSI topologies: input voltage and current (a) and DC-link voltage and current (b)

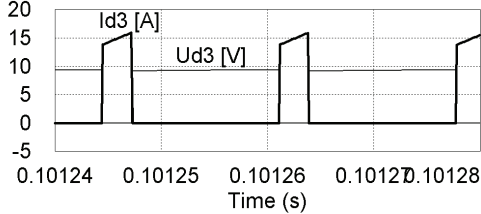


Fig. 10. Operating voltage and current of diode D_3

Comparison of Idealized Boost Properties of Proposed Topologies. By the help of simulations it was verified (Fig. 11) that the capacitor assisted and diode assisted qZSI have common advantages, such as continuous input current and increased boost factor of the input voltage for the same value of the shoot-through duty cycle as with the traditional qZSI [1-3]. Moreover, in the lossless approach the CAEB and MCAEB qZSI topologies could ensure up to 1.25 times higher boost than that of DAEB and MDAEB qZSI topologies (Fig. 11).

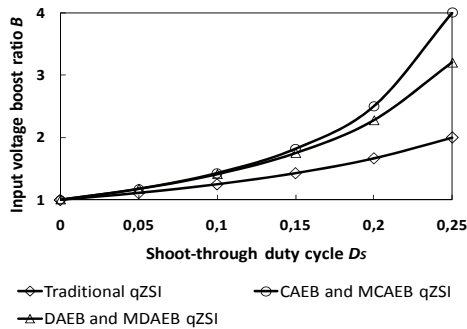


Fig. 11. Comparison of idealized boost properties of capacitor assisted and diode assisted extended boost qZSIs

Experimental Results

In order to verify theoretical assumptions the laboratory setups corresponding to the investigated topologies were assembled. 600 V/200 A IGBT with extra low saturation voltage was selected for S (see Fig. 3 for the details). Components used in the qZS-networks had the following properties:

$$\begin{aligned} L_1 \dots L_3 &= 50 \text{ uH}; R_L = 3 \text{ m}\Omega; \text{ type: toroidal inductors;} \\ C_1 \dots C_4 &= 180 \text{ uF}; \text{ type: polypropylene capacitors;} \\ D_1 \dots D_3 &= 100 \text{ V}/80 \text{ A power Schottky diodes.} \end{aligned}$$

In the first experiment, main operating waveforms of the proposed topologies were acquired and compared. The shoot-through duty cycle was set at 0.167. As seen from Fig. 12b, due to the losses in the components of the qZS-network both of the capacitor assisted topologies could

provide only a 90% of a theoretically predicted input voltage gain (DC-link voltage amplitude 54 V instead of 60 V). In the case of diode assisted topologies (Fig 13b) the practical voltage gain for the same operating conditions was reduced by 9% in comparison with the theoretically predicted (DC-link voltage amplitude 52 V instead of 57 V). Due to the input inductor L_1 all the proposed topologies feature the continuous input current in the CCM, as predicted in the analysis.

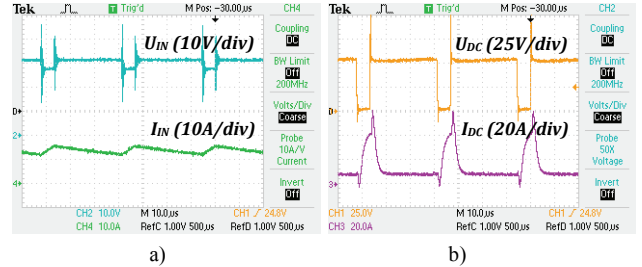


Fig. 12. Experimental waveforms of input voltage and current (a) and DC-link voltage and current (b) of the CAEB and MCAEB qZSIs

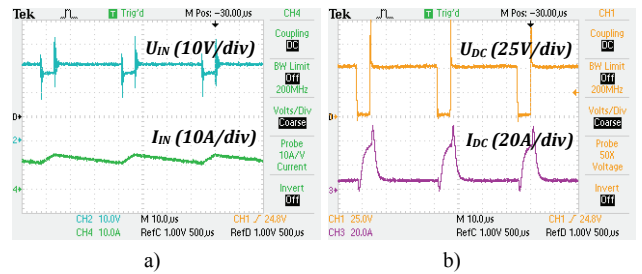


Fig. 13. Experimental waveforms of input voltage and current (a) and DC-link voltage and current (b) of the DAEB and MDAEB qZSIs

During the second experiment the boost properties of the proposed topologies were experimentally verified and compared with theoretical results. In the conditions of fixed input voltage (30 V) and constant load (5 Ω), the shoot-through duty cycle of the converters was increased step by step from 0 to 0.25.

Fig. 14 shows that all of the presented topologies suffer from the boost factor reduction, which is mostly caused by the losses in the inductors and diodes of the qZS-network as well as by voltage drops in the interconnection wires. In order to achieve higher possible voltage gain and efficiency these problematic issues should be first addressed during the design routine of extended boost qZS-converters.

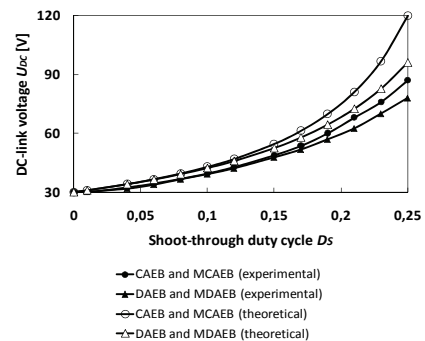


Fig. 14. Theoretical and practical boost properties of the compared topologies

Another interesting fact is that all four topologies have demonstrated identical boost properties within the shoot-through duty cycle range of 0...0.15, which could be considered during proper topology selection for different applications.

Conclusions

In this paper four extended boost qZSI topologies were proposed, discussed and compared. These topologies were classified as capacitor assisted and diode assisted. A steady state analysis of topologies operating in the continuous conduction mode was performed. Theoretical study was validated by the simulations and experiments.

It was experimentally stated that in similar operating conditions the discussed topologies provide an identical boost factor of the input voltage within the shoot-through duty cycle range of 0...0.15. Thanks to the presence of the input inductor L_I all the discussed extended boost qZSIs have continuous input current in the CCM, thus featuring the reduced stress of the input voltage source.

Acknowledgment

This research has been supported by Estonian Ministry of Education and Research (Project SF0140016s11) and Estonian Science Foundation (Grant ETF8538).

References

1. **Anderson J., Peng F. Z.** Four quasi-Z-Source inverters // IEEE Power Electronics Specialists Conference (PESC'2008), 2008. – P. 2743–2749.
2. **Yuan Li, Anderson J., Peng F. Z., Dichen Liu.** Quasi-Z-Source Inverter for Photovoltaic Power Generation Systems // Twenty-Fourth Annual IEEE Applied Power Electronics Conference and Exposition (APEC'09), 2009. – P. 918–924.
3. **Jong-Hyoung Park, Heung-Geun Kim, Eui-Cheol Nho, Tae-Won Chun, Jaeho Choi.** Grid-Connected PV System Using a Quasi-Z-Source Inverter // Twenty-Fourth Annual IEEE Applied Power Electronics Conference and Exposition (APEC'09), 2009. – P. 925–929.
4. **W.-Toke Franke, Malte Mohr, Friedrich W. Fuchs** Comparison of a Z-Source Inverter and a Voltage-Source Inverter Linked with a DC/DC Boost-Converter for Wind Turbines Concerning Their Efficiency and Installed Semiconductor Power // IEEE Conf. (PESC'08), 2008. – P. 1814–1820.
5. **Gajanayake C. J., Luo F. L., Gooi H. B., So P. L., Siow L. K.** Extended boost Z-source inverters // IEEE Conf. (ECCE'09), 2009. – P. 3845–3850.
6. **Adamowicz M., Strzelecki R., Vinnikov D.** Cascaded Quasi-Z-Source Inverters for Renewable Energy Generation Systems // Ecologic Vehicles and Renewable Energies Conference (EVER'10), 2010.
7. **Vinnikov D., Roasto I., Strzelecki R., Adamowicz M.** Performance Improvement Method for the Voltage-Fed qZSI with Continuous Input Current // IEEE Mediterranean Electrotechn. Conf. (MELECON'10), 2010.
8. **Vinnikov D., Roasto I., Jalakas T.** Comparative Study of Capacitor-Assisted Extended Boost qZSIs Operating in CCM // 12th Biennial Baltic Electronic Conf. BEC'2010, 2010.
9. **Knyva V., Knyva M.** Algorithm for Estimation of Measurement Devices Software's Metrological Reliability // Electronics and Electrical Engineering. – Kaunas: Technologija, 2010. – No. 4(100). – P. 47–50.

Received 2011 02 02

D. Vinnikov, I. Roasto, T. Jalakas, S. Ott. Extended Boost Quasi-Z-Source Inverters: Possibilities and Challenges // Electronics and Electrical Engineering. – Kaunas: Technologija, 2011. – No. 6(112). – P. 51–56.

In this paper four new extended boost qZSIs with continuous input current were presented, analyzed and compared. Moreover, some problematic issues of these converters were pointed out and discussed. Theoretical background was verified by the simulations and experiments. III. 14, bibl. 9, tabl. 1 (in English; abstracts in English and Lithuanian).

D. Vinnikov, I. Roasto, T. Jalakas, S. Ott. Išplėstinių qZS keitiklių galimybės // Elektronika ir elektrotechnika. – Kaunas: Technologija, 2011. – Nr. 6(112). – P. 51–56.

Pristatomi nauji išplėstiniai qZS keitikliai. Atlikta keitiklių su nuolatine įėjimo srove analizė bei palyginimas. Pateiktos kai kurios keitiklių problemos. Buvo atliktas matematinis modeliavimas ir eksperimentiniai tyrimai. II. 14, bibl. 9, lent. 1 (anglų kalba; santraukos anglų ir lietuvių k.).